Int. J. Solids Structures Vol. 22, No. 2, pp. 121–134, 1986
Printed in Great Britain.

0020–7683/86 $3.00 + .00

ON CRACK-TIP STRESS STATE: AN EXPERIMENTAL EVALUATION OF THREE-DIMENSIONAL EFFECTS

ARES J. ROSAKIS† and K. RAVI-CHANDAR‡
Graduate Aeronautical Laboratories, California Institute of Technology, Pasadena, CA 91125, U.S.A.

(*Received* 28 *April* 1984; *in revised form* 22 *March* 1985)

Abstract—The extent of the region of three-dimensionality of the crack-tip stress field is investigated using reflected and transmitted caustics. The range of the applicability of two-dimensional near tip solutions is thus established experimentally. The experiments are performed using Plexiglass and high-strength 4340-steel compact tension specimens. A wide spectrum of thicknesses is investigated. At each thickness, measurements are performed at a variety of distances r from the crack tip, ranging from $r/h = 0$ to $r/h = 2$, where h is the specimen thickness. The results indicate that plane-stress conditions prevail at distances from the crack tip greater than half the specimen thickness, while *no* significant plane-strain region is detected. The experimental results are also compared to the crack-tip boundary-layer solution of Yang and Freund[1], and the numerical results of Levy, Marcal and Rice[2]. Their solutions are consistent with the results of this work and approach the plane stress field at $r/h = 0.5$. In addition, and unlike what might be commonly expected, the analytical solution[1] exhibits no plane-strain behavior very near the crack tip. This behavior is in good agreement with the results of both the transmission and the reflection experiments.

1. INTRODUCTION

It has long been recognized that in plates of finite thickness, the stress field at the vicinity of stress raisers is three-dimensional in nature. The problem of a hole in an infinite plate has been successfully addressed in the works of Sternberg and Sadowsky[3] and Alblas[4]. The more complex problem of a crack in a thick plate has been attempted by a number of authors[5–8], but no complete solution has been obtained as yet.

The purpose of this paper is not to solve this complex problem in detail, but rather to explore regions where two-dimensional approximations would be acceptable. In particular, we attempt to identify the regions in which local experimental measurements based on two-dimensional theory can be performed with confidence. Such local measurements are based on the use of photoelasticity, interferometry or caustics (shadowgraphy), where data are usually obtained at some characteristic distance r from the tip. The constraint on the location of r, if a two-dimensional view point is adopted, is the existence of a K-dominant field (negligible high-order term effects and contained yielding). However, in plates of finite thickness, three-dimensional effects near the tip must assume a role at least as important as the above constraints. In the sequel such three-dimensional effects were investigated for Plexiglas in transmission and 4340 steel in reflection, using the optical method of caustics.

Recently, Yang and Freund[1], motivated by similar concerns regarding experimental measurements made in the vicinity of the crack tip, have explored the three-dimensional crack problem using a boundary-layer approach. Their analytical results have a close relationship to the present investigation, and will be compared in detail in Section 5. Also, the numerical results of the same problem presented by Levy, Marcal and Rice[2] will be compared with experiment.

† Assistant Professor, Graduate Aeronautical Laboratories, California Institute of Technology, Pasadena, CA 91125, U.S.A.
‡ Formerly, Research Fellow, Caltech. Assistant Professor, Department of Mechanical Engineering, University of Houston, TX 77004, U.S.A.

2. THEORETICAL CONSIDERATIONS

Consider a semi-infinite mode-I crack in a homogeneous isotropic linear-elastic solid of uniform undeformed thickness h. The crack is assumed to be mathematically sharp with a straight crack front. If a local Cartesian coordinate system is introduced at the crack with its origin situated at the middle of the crack front (see Fig. 1), then the stress field at the vicinity of the crack tip can be expressed as a function of the dimensionless coordinates x_3/h, r/h, as well as the angular variation ϑ. In particular

$$\boldsymbol{\sigma} = \boldsymbol{\sigma}(x_3/h, r/h, \vartheta), \tag{2.1}$$

where $r^2 = x_1^2 + x_2^2$, $\vartheta = \tan^{-1}(x_2/x_1)$.

The choice of h as a normalization parameter is dictated by the observation that, for the problem considered, the thickness is the only relevant length scale. In addition, expression (2.1) must be such as to reduce to the familiar two-dimensional singular asymptotic stress field when conditions of either plane stress or plane strain are approached. More specifically, the value of the nondimensional variable r/h must reflect the changing nature the stress field as the crack front is approached from infinity. For $r/h \to \infty$, plane-stress–like conditions are expected to prevail—this being true for either very thin specimens and/or for large distances from the crack line. Also for $r/h \to 0$, and $x_3/h \neq \pm \frac{1}{2}$, a plane-strain type of field is expected to dominate†—this being true for either thick specimens and/or small distances from the crack line. Thus, in general,

$$\boldsymbol{\sigma} = \boldsymbol{\sigma}(x_3/h, r/h, \vartheta) \to \frac{K_{2D}}{\sqrt{2\pi r}} \cdot \mathbf{f}(\vartheta) \begin{cases} K_{2D} & \text{for } r/h \to \infty \\ K_E & \text{for } r/h \to 0 \end{cases}, \tag{2.2}$$

where K_{2D} and K_E are the mode-I plane-stress and plane-strain stress-intensity factors, respectively, and $\mathbf{f}(\vartheta)$ is a tensor function of ϑ, completely determined by the two-dimensional asymptotic near-tip analysis[9]. The region near the tip, where r/h is neither very large nor very small, is in general an area where three-dimensional effects are expected to be very strong. This region becomes particularly important in fracture mechanics for the following two reasons: First, from the theoretical point of view, accurate solutions describing the stress behavior there have been particularly elusive. Second, from the experimental point of view, it seems that despite its great three-

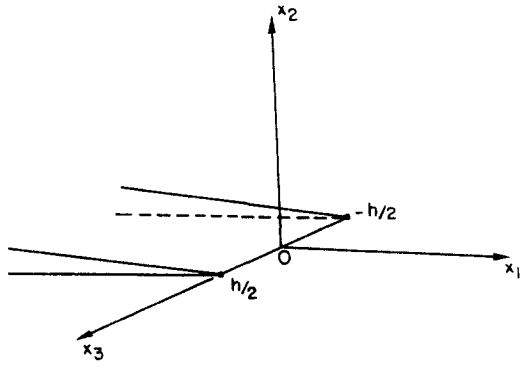

Fig. 1. Semi-infinite crack in plate of thickness h.

† As $r/h \to 0$ and $x_3/h = \pm \frac{1}{2}$ (points on specimen surface near the crack front) the nature of the singularity deviates from its two-dimensional nature due to the existence of a free corner there[5–7]. On the other hand, for $x_3/h \neq \pm \frac{1}{2}$ (points inside the specimen) conditions of plane strain are expected to dominate if the crack front is approached close enough.

dimensionality, this region has been selected in a number of experiments as a site of measurements, unfortunately interpreted on the basis of two-dimensional solutions.

In this work we will not attempt the solution of the very complicated three-dimensional problem. Instead, we have chosen to investigate the size of the annular zone of three-dimensional effects. In order to do so, we have introduced a couple of simplifying assumptions, which do not affect the three-dimensional nature of the field. Our assumptions do not predict the detailed character of the three-dimensional state, and have been introduced on the basis of qualitative preliminary experimental observations, which will be discussed later.

In particular we have assumed that the components of the stress field can be expressed as follows:

$$\begin{aligned}
\sigma_{\alpha\beta} &= K_1(x_3/h,\, r/h)\cdot\frac{1}{\sqrt{2\pi r}}\cdot\Sigma_{\alpha\beta}(\vartheta),\\
\sigma_{\alpha 3} &= K_2(x_3/h,\, r/h)\cdot\frac{1}{\sqrt{2\pi r}}\cdot\Sigma_{\alpha 3}(\vartheta),\\
\sigma_{33} &= K_3(x_3/h,\, r/h)\cdot\frac{1}{\sqrt{2\pi r}}\cdot\Sigma_{33}(\vartheta),
\end{aligned} \tag{2.3}$$

where $K_i(x_3/h,\, r/h)$, $i = 1, 2, 3$ are unknown functions of x_3/h and r/h. In eqns (2.3), and in the remaining paper, Greek indices will have the range 1, 2.

Expressions (2.3) assume that only the ϑ dependence is separable, and do *not* provide any information concerning the nature of the r/h dependence of the stress field.

The separability of the ϑ dependence, as well as the requirement that expressions (2.3) reduce to eqns (2.2) for $r/h \to 0$ and $r/h \to \infty$, imply that

$$\begin{aligned}
\Sigma_{11} &= f_{11} = \cos\frac{\vartheta}{2}\,[1 - \sin\vartheta/2 \sin 3\vartheta/2],\\
\Sigma_{22} &= f_{11} = \cos\frac{\vartheta}{2}\,[1 + \sin\vartheta/2 \sin 3\vartheta/2], \qquad \forall r/h,\\
\Sigma_{12} &= f_{12} = \sin\vartheta/2 \cos\vartheta/2 \cos 3\vartheta/2,\\
\Sigma_{33} &= f_{33} = 2\nu \cos\vartheta/2.
\end{aligned} \tag{2.4}$$

Also for the plane-stress limit, as $r/h \to \infty$, $K_{1,3}(x_3/h,\, r/h) \to K_{2D}$ and $K_2(x_3/h,\, r/h) \to 0$. And that for the plane-strain limit, as $r/h \to 0$, $K_1(x_3/h,\, r/h) \to K_E$ and $K_{2,3}(x_3/h,\, r/h) \to 0$. Thus the governing equations can be written as

$$\begin{aligned}
\sigma_{\alpha\beta} &= K_{2D}\hat{K}_1(x_3/h,\, r/h)\,\frac{f_{\alpha\beta}(\vartheta)}{\sqrt{2\pi r}},\\
\sigma_{\alpha 3} &= K_{2D}\hat{K}_2(x_3/h,\, r/h)\,\frac{f_{\alpha 3}(\vartheta)}{\sqrt{2\pi r}},\\
\sigma_{33} &= K_{2D}\hat{K}_3(x_3/h,\, r/h)\,\frac{f_{33}(\vartheta)}{\sqrt{2\pi r}},
\end{aligned} \tag{2.5}$$

where

$$\hat{K}_i(x_3/h,\, r/h) = \frac{K_i(x_3/h,\, r/h)}{K_{2D}}.$$

3. THE METHOD OF CAUSTICS

Physical principle

Consider a family of light rays parallel to the x_3 axis, incident on a planar specimen whose midplane lies at $x_3 = 0$ (cf. Fig. 2). Upon reflection from an opaque specimen, or refraction through a transparent specimen, the rays undergo an optical path change dictated by the stress field, and in general will deviate from parallelism. Under certain stress gradients, the reflected or refracted rays will form an envelope in the form of a three-dimensional surface in space. This surface, which is called the *caustic surface*, is the locus of points of maximum luminosity in the reflected or transmitted light fields. The deflected rays are tangent to the caustic surface. If a screen is positioned parallel to the $x_3 = 0$ plane, and so that it intersects the caustic surface, then the cross-section of this surface can be observed as a bright curve (the so-called *caustic curve*) bordering a dark region (the *shadow spot*) on the screen. Suppose that the incident ray, which is reflected from or transmitted through point $p(x_1, x_2)$ on the specimen, intersects the screen at the image point $P(X_1, X_2)$ (cf. Fig. 2.). The X_1, X_2 coordinate system is identical to the x_1, x_2 system, except that the origin of the former has been translated the distance z_0 to the screen (z_0 can be either positive or negative). The position of the image-point P will depend on the gradient of the optical path change ΔS, introduced by the medium and on the distance z_0, and is given by [10]

$$X_i = x_i \pm z_0 \frac{\partial(\Delta S)}{\partial x_i}. \tag{3.1}$$

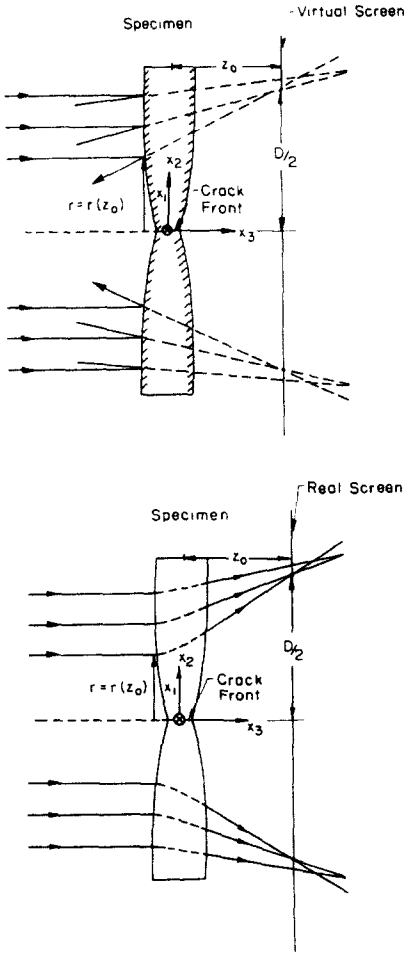

Fig. 2. Schematic of the formation of the caustics by (a) reflection and (b) transmission.

For the reflection case, $\Delta S = -2u_3(x_1, x_2, h/2)$ where u_3 is the displacement in the x_3 direction.

Equation (3.1) is a mapping of the points on the specimen onto points of the screen. If the screen intersects the caustic surface, then the resulting caustic curve on the screen is a locus of points of multiple reflection. That is, for points on the caustic curve, the mapping (3.1) is not invertible and the determinant of the Jacobian matrix of the transformation must vanish, i.e.

$$J(x_1, x_2; z_0) = \frac{\partial(X_1, X_2)}{\partial(x_1, x_2)} = 0. \tag{3.2}$$

Equation (3.2) is the necessary and sufficient condition for the existence of a caustic curve. The points on the specimen for which the Jacobian vanishes are the points from which the rays forming the caustic curve emerge. These rays are tangent to the caustic surface at its intersection with the plane of the screen. The locus of the points on the specimen mapped onto the caustic curve is called the *initial curve*. Equation (3.2) describes the initial curve and its strong parametric dependence on z_0. Rays emerging from within the initial curve map outside the caustic curve, and therefore only the rays emerging from the initial curve determine the geometry of the caustic curve. This characteristic of the optical mapping is vital to this work. By varying the position z_0 of the screen, the size of the initial curve (radius r) is varied. Thus the near-tip topology can be investigated at various distances r from the crack tip.

Caustics by reflection

For opaque specimens, caustics are formed by the reflection of light rays from the highly polished specimen surface. The shape of the caustic curve depends on the near-tip normal displacement u_3 of the plate face initially at $x_3 = h/2$, which is given by

$$u_3(x_1, x_2, h/2) = h \int_0^{1/2} \epsilon_{33}(x_1/h, x_2/h, x_3/h)\, \mathrm{d}(x_3/h).$$

where ϵ_{33} is the direct strain in the thickness direction. For a linearly elastic solid,

$$\epsilon_{33} = \frac{1}{E}[\sigma_{33} - \nu(\sigma_{11} + \sigma_{22})], \tag{3.3}$$

and thus using (2.5),

$$u_3(r/h, \vartheta, h/2) = \frac{2h\nu K_{2D}}{E\sqrt{2\pi r}}\, \rho(r/h) \cos(\vartheta/2) \tag{3.4}$$

where

$$\rho(r/h) = \int_0^{1/2} [\hat{K}_3(x_3/h, r/h) - \hat{K}_1(x_3/h, r/h)]\, \mathrm{d}(x_3/h) \equiv \frac{K^{\mathrm{EXP}}(r/h)}{K_{2D}}.$$

We have chosen to denote the function $K_{2D}\rho(r/h)$ as K^{EXP}, since it may be possible to measure this quantity for different values of r/h. Appropriate variations of z_0 allow us to obtain initial curves at different distances r from the crack tip.

Caustic by transmission

For transparent specimens the optical path change ΔS depends on both local changes in thickness and on local changes of refractive index, and can be expressed

in a manner similar to the two-dimensional case in [10] as

$$\Delta S(x_1, x_2) = 2(n-1)h \int_0^{1/2} \epsilon_{33}\, \mathrm{d}(x_3/h) + 2h \int_0^1 \Delta n\, \mathrm{d}(x_3/h), \tag{3.5}$$

where the change in refractive index Δn is given by

$$\Delta n = A(\sigma_{11} + \sigma_{22} + \sigma_{33}),$$

and where A is the stress-optic constant[10]. Substituting the above together with (2.5) and (3.3) into (3.5) gives

$$\Delta s(r/h, \vartheta) = \frac{2hc_\sigma K_{2D}}{\sqrt{2\pi r}}\, \rho'(r/h) \cos \vartheta/2, \tag{3.6}$$

where

$$\rho'(r/h) = \int_0^{1/2} \left(\hat{K}_1(x_3/h, r/h) + \frac{\xi}{c_\sigma} \hat{K}_3(x_3/h, r/h) \right) \mathrm{d}(x_3/h) \equiv \frac{K^{\mathrm{EXP}}(r/h)}{K_{2D}},$$

and

$$c_\sigma = \left[A - (n-1)\frac{\nu}{E} \right], \qquad \text{plane-stress optical constant,}$$

$$\xi = \left[(n-1)\frac{\nu}{E} + A\nu \right].$$

Evaluation of the mapping

Substituting eqn (3.4) or (3.6) into the equation of the mapping (3.1), one obtains

$$\begin{aligned} X_1 &= r\cos\vartheta + \gamma K^{\mathrm{EXP}} r^{-3/2} \cos 3\vartheta/2 + \gamma \frac{\partial K^{\mathrm{EXP}}}{\partial r} r^{-1/2} \cos \vartheta/2 \cos\vartheta, \\ X_2 &= r\sin\vartheta + \gamma K^{\mathrm{EXP}} r^{-3/2} \sin 3\vartheta/2 + \frac{\gamma \partial K^{\mathrm{EXP}}}{\partial r} r^{-1/2} \sin \vartheta/2 \sin\vartheta, \end{aligned} \tag{3.7}$$

where

$$\gamma = \begin{cases} \dfrac{z_0 \nu h}{(2\pi)^{1/2} E}, & K^{\mathrm{EXP}} = \rho(r/h) K_{2D} \quad \text{for reflection,} \\ \dfrac{z_0 c_\sigma h}{(2\pi)^{1/2}}, & K^{\mathrm{EXP}} = \rho'(r/h) K_{2D} \quad \text{for transmission.} \end{cases}$$

The first two terms of the right-hand side are the traditional two-dimensional caustic terms.

The presence of the third term should alter the geometry of the caustic curve and therefore the relation between $K^{\mathrm{EXP}}(r/h)$ and the dimensions of the caustic. However, extensive experimental observations of the caustic geometry (in particular, the aspect ratio) have demonstrated that the epicycloidal shape expected on the basis of the first two terms is retained (cf. Fig. 3). The photographs in Fig. 3 demonstrate that despite drastic changes in r/h, the caustic-curve shape remains unchanged. This suggests that the effect of the third term in expression (3.7) must be small compared to the second

(a)

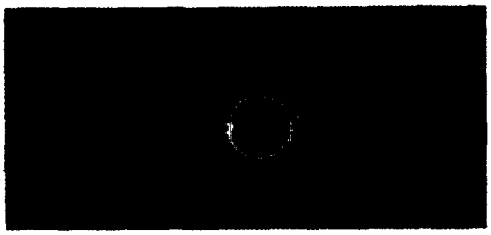

(b)

Fig. 3. Comparison of two caustic-curve shapes obtained at different distances from the crack tip. Both photographs correspond to the same experiment: (a) $r/h = 0.9$; (b) $r/h = 0.15$

term. This means that the ratio of the two terms is small, implying that

$$\frac{1}{K^{\mathrm{EXP}}}\frac{\partial K^{\mathrm{EXP}}}{\partial r} = o\left(\frac{1}{r}\right) \qquad \text{as} \quad r \to 0. \tag{3.8}$$

Assuming the validity of eqn (3.8), one recovers from eqn (3.7) the traditional caustic equations, with the exception that the experimentally determined stress intensity K^{EXP} now varies with r/h. The caustic curve is then an epicycloid, and the "initial curve" is a circle of radius r. The radius of the initial curve r depends on the choice of z_0, and was varied during the experiment. By changing z_0, a number of optical measurements were performed at different distances from the crack tip.

The initial curve

As noted earlier in this section, the condition for the existence of a caustic curve on a screen at $x_3 = z_0$, is the vanishing of the Jacobian of the transformation (3.7). With reference to eqn (3.2), and assuming the validity of eqn (3.8), the condition that the determinant of the Jacobian matrix must vanish becomes

$$J = r - \left(\frac{3}{2}\gamma K^{\mathrm{EXP}}\right)^{2/5} \tag{3.9}$$

Equation (3.9) describes the initial curve on the specimen surface. Then substitution of eqn (3.9) into eqn (3.7) yields the equation of the corresponding caustic curve in the X_1, X_2 plane, parametric in angle ϑ. For the case under consideration, the equation of the caustic curve becomes

$$\begin{aligned} X_1 &= r[\cos\vartheta + 2/3\cos 3\vartheta/2], \\ X_2 &= r[\sin\vartheta + 2/3\sin 3\vartheta/2], \\ &\quad -\pi < \vartheta < \pi, \end{aligned} \tag{3.10}$$

where r is constrained by eqn (3.9). Equation (3.10) is the equation of an epicycloid, whose shape remains unchanged as r is varied. This result was confirmed (see Fig. 3) during the experiment, and thus assumption (3.8) was justified.

On the other hand, the absolute size of the caustic curve depends on the value of K^{EXP}, the bulk material properties, z_0, and the optical constants. In fact, eqn (3.10) is a relationship among all of these parameters. Thus if the values of the material, geometrical and optical parameters are known, then eqn (3.10) provides a relationship between the size of the caustic curve and the local value of K^{EXP}. Adopting the maximum transverse diameter $D/2 = \max(X_2)$ as the characteristic dimension of the caustic curve, the value of K^{EXP}, measured at a distance r (initial-curve radius) from the crack tip, can be expressed as

$$K^{EXP} = \frac{9.34 \times 10^{-2} D^{5/2}}{z_0 ch}, \tag{3.11}$$

where

$$c = \begin{cases} c_\sigma & \text{for transmission,} \\ \nu/E & \text{for reflection.} \end{cases}$$

Also, from eqns (3.9) and (3.11), it can be demonstrated that the maximum transverse diameter of the caustic is related to the radius of the initial curve by the formula

$$D = 3.163r. \tag{3.12}$$

4. EXPERIMENTAL CONSIDERATIONS

In order to undertake an experimental investigation of thickness effects, careful experiments have to be designed so as to isolate this effect from other geometry-related effects on the stress field. This requirement implies that the only length scale in the problem is the thickness, or, equivalently, that the in-plane dimensions be large in comparison to the thickness. However, cost considerations limit the in-plane dimensions, especially when large thicknesses are involved and a compromise between the more important mechanics considerations and cost essentially dictates the sizes of the specimens. The final choice of specimen geometry is illustrated in Fig. 4. Two materials were chosen for these experiments. Plexiglas was selected for investigation in transparent cases because of its easy availability in various thicknesses. For investigating opaque specimens, a 4340 martensitic steel, heat treated to 843°C and oil quenched, was selected because its high yield strength precluded plasticity effects that might hinder the thickness-effect investigation.

The plane stress-intensity factor for the geometry shown in Fig. 4 can be obtained from analysis, and is given by [11]

$$K_{2D} = \frac{P\sqrt{a}}{h} F_1\left(\frac{a}{b}, \frac{l}{b}, \frac{d}{l}\right). \tag{4.1}$$

where F_1 is a function of crack length a, ligament length d, specimen height l, and the distance between loading points $2d$. Also, P is the applied load. This value of K_{2D} will be used in the sequel to compare with the experimentally determined values of the stress-intensity factor, K^{EXP}. The method of caustics is used to determine the value of K^{EXP}. The analytical basis for the use of the traditional caustics relations has been discussed in Section 3. Thus

$$K^{EXP} = \frac{9.34 \times 10^{-2}}{z_0 ch} D^{5/2}, \tag{4.2}$$

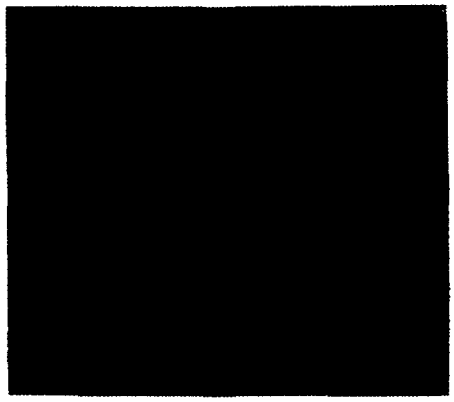

(a)

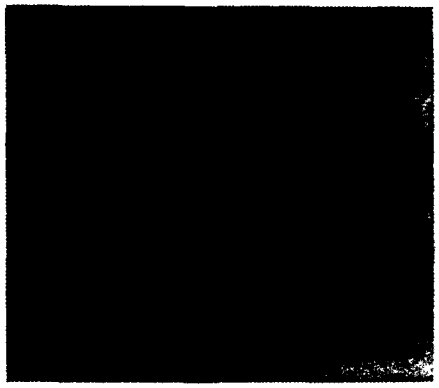

(b)

Fig. 4. The specimen geometry: (a) Plexiglas; (b) flat and highly polished Martensitic 4340 carbon steel.

where z_0 is the reference distance, h is the plate thickness, D is the maximum transverse diameter of the caustic, and c is the appropriate optical constant: c_σ for plane stress, c_ϵ for plane strain, or ν/E for reflection. D is related to the initial-curve radius r by the formula $D = 3.163\, r$, see Section 3.

Two sets of experiments were performed: the first set with transparent Plexiglas, and the second set with martensitic 4340 steel. For the Plexiglas experiments, the plane-stress value of $c = c_\sigma = 1.08 \times 10^{-10}$ m^2/MN[10] was used in evaluating K^{EXP}. For the steel specimen, the value of $c = \nu/E$, where ν is the Poisson's ratio, and E is the Young's modulus. In these two sets of experiments, there is a fundamental difference in the way that information is extracted experimentally. In Plexiglas, the light rays travel through the specimen and emerge with the integrated effect of the stress field in the specimen. Whereas in the opaque specimen, the strain ϵ_{33} accumulates through the thickness, thereby presenting a dimpled surface from which light rays reflect to form the caustic curve. In other words, the Plexiglas experiments provide an optically-averaged value of K^{EXP}, and the 4340-steel experiments give a materially-averaged value of K^{EXP}. However, since both materials have similar Poisson's effect, one might reasonably expect that the thickness effects in the two cases might present similarities.

The specimen preparation was a major part of the whole experiment. While the exterior geometry is easily machined, achieving proper crack-tip conditions is of primary importance. In order to compare the experimental results obtained for various thicknesses, the crack front must not possess any curvature. This was easily achieved in steel specimens where the crack was made using an EDM spark-cutter. The metallic specimen is shown in Fig. 4(a). For the Plexiglas specimens, after a lot of trial and error, it was found that the best way of producing straight crack fronts was to start with a machined Chevron notched crack front and grow the crack front under quasi-

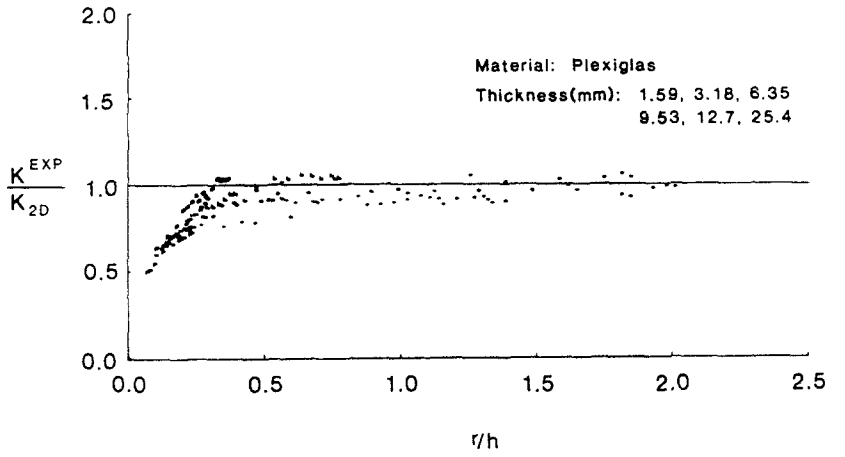

Fig. 5. Ratio of stress-intensity factor inferred from local shadow spot measurements (transmitted caustics) to analytical two-dimensional value, vs distance from crack tip divided by specimen thickness. Material: Plexiglas.

static conditions, rather than cyclic loading conditions. The resulting crack front from a specimen of 6.35-mm thickness is shown in Fig. 4(b).

In order to use the method of caustics in an opaque material, the undeformed surface of the specimen has to be a flat reflector. This was achieved by grinding, lapping and polishing the specimen to have a half-a-wavelength surface flatness. For Plexiglas, no special surface preparation was necessary. In the experiment, a collimated laser beam passes through the specimen thickness in the transparent case and reflects from the deformed surface in the opaque case. Due to the specimen deformation, the originally collimated light beam forms a caustic surface, as discussed in Section 3. A camera is focused on a plane at a distance z_0 from the specimen, and the caustic curve on that plane is photographed. From the diameter of the caustic, the stress-intensity factor is calculated using eqn (4.2). This corresponds to making a measurement at a distance r from the crack tip, where r is the initial-curve radius. Since there are no light rays inside the caustic surface (cf. Fig. 2), this implies that the light rays that pass through the specimen at radii less than r do not provide any information in this reference plane. Therefore, by varying the distance z_0, it is seen from Fig. 2 that measurements of K^{EXP} may be made at various distances r from the crack tip. This is easily done by changing the plane-of-focus of the camera. However, in order to retain the same magnification, the camera itself was moved to obtain different z_0 and r values.

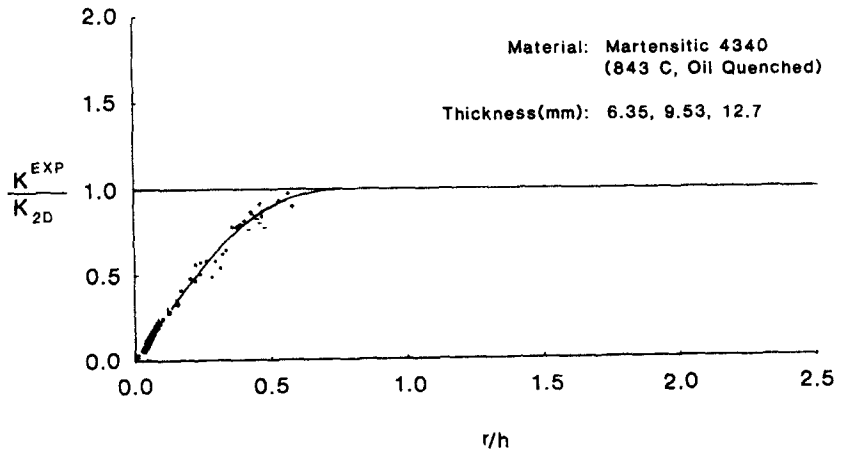

Fig. 6. Ratio of stress-intensity factor inferred from local shadow spot measurements (reflected caustics) to analytical two-dimensional value, vs distance from crack tip divided by specimen thickness. Material: Martensitic 4340 carbon steel.

Plexiglas specimens, of thicknesses 1.59–25.4 mm, were tested in an Instron loading machine at loads varying from 100 to 250 N. The z_0 distance was varied between 0.005 and 10 m. This resulted in a r/h variation from about 0.01 to 2. The results are plotted in normalized variables. The experimentally obtained K^{EXP} is normalized by K_{2D} and plotted as a function of r/h in Fig. 5 for Plexiglas. Three thicknesses (6.35, 9.53 and 12.7 mm) of the 4340 steel were tested in reflection at loads varying from 1 to 16 KN. The ratio of r/h was varied from about 0 to 0.6. In the reflection arrangement, increasing r/h above 0.6 proved to be increasingly difficult due to limitations in the experimental arrangement. The experimental results of K^{EXP}/K_{2D} are plotted as a function of r/h in Fig. 6.

5. DISCUSSION

The most striking feature of the experimental results displayed in Figs. 5 and 6 is the r/h similarity. In particular, the Plexiglas results contain data from 12 different tests using six thicknesses. Each of the tests covers different but overlapping range of r/h. In all cases, the K^{EXP}/K_{2D} exhibits the same r/h dependence. Also, in the case of the 4340 steel, r/h is the scaling parameter. This common r/h dependence will be referred to here as the "master curve", which, however, is different in transmission and reflection. Furthermore, it is clear from both the curves that for $r/h > 0.5$, K^{EXP} approaches K_{2D}. Since a plane-stress caustics analysis was used in evaluating K^{EXP}, and in view of the r/h similarity, it is apparent that *plane-stress conditions prevail at distances from the crack tip which are greater than half the specimen thickness.*

For $r/h < 0.5$, three-dimensional effects seem to take over and the validity of a two-dimensional analysis becomes questionable. Moreover, experimental measurements based on two-dimensional analyses, if performed at $r/h < 0.5$, are likely to contain large errors which increase as r/h decreases. The usual practice has been to make local measurements at very small distances from the tip, to ensure a K-dominant two-dimensional asymptotic field (implying negligible higher-order term effects). As demonstrated in Fig. 5, *the error due to the three-dimensional effects in the near-tip region* ($r/h < 0.5$) *seems to be more important than the neglect of higher-order terms in the far field* ($0.5 < r/h < 2.0$), where the plane-stress result seems to be valid.

The existence of a region with strong three-dimensional effects is not surprising, and was anticipated in Section 2. Also, as r/h decreases, a plane-strain regime is expected, particularly on the basis of plane-strain fracture toughness concepts. The results displayed in Fig. 5 and 6 ought to identify the extent of a plane-strain region. In transmission K^{EXP}/K_{2D} must tend to the ratio of $c_\epsilon/c_\sigma < 1$, since the plane-stress analysis of caustics was used. The master curve of Fig. 5 shows that K^{EXP}/K_{2D} is continuously decreasing below $c_\epsilon/c_\sigma = 0.7$, instead of reaching a constant value over a substantial range of r/h. This demonstrates that *the region where plane-strain conditions are likely to prevail is surprisingly small.* In reflection, K^{EXP}/K_{2D} must tend to zero under plane-strain conditions, since reflections from a flat surface will not produce a caustic ($\partial u_3/\partial r = 0$). In Fig. 6, it is seen that K^{EXP}/K_{2D} indeed goes to zero, but *not* over a significant range of r/h (i.e. it goes to zero only right at the crack tip). This is consistent with the results of transmission in indicating that the extent of the possible plane-strain region is *small.*

To graphically illustrate the consequences of the experimental result in the reflecting specimen, Fig. 6 was replotted in terms of the variation of $u_3(r/h, \vartheta = 0, x_3 = h/2)$ as a function of r/h, using eqn (3.4). This provides the profile of the deformed-specimen surface at the vicinity of the tip. This profile is plotted in Fig. 7. It demonstrates that deviations from the plane-stress solution occur for $r/h = 0.5$. This deviation can be expected on the grounds that the plane-stress solution predicts a physically unacceptable unbounded displacement u_3 as $r/h \to 0$.

As r/h decreases below 0.5, a minimum in the displacement profile is indicated at $r/h = 0.4$. For $r/h \to 0$, the present experimental results displayed in Fig. 7 indicate

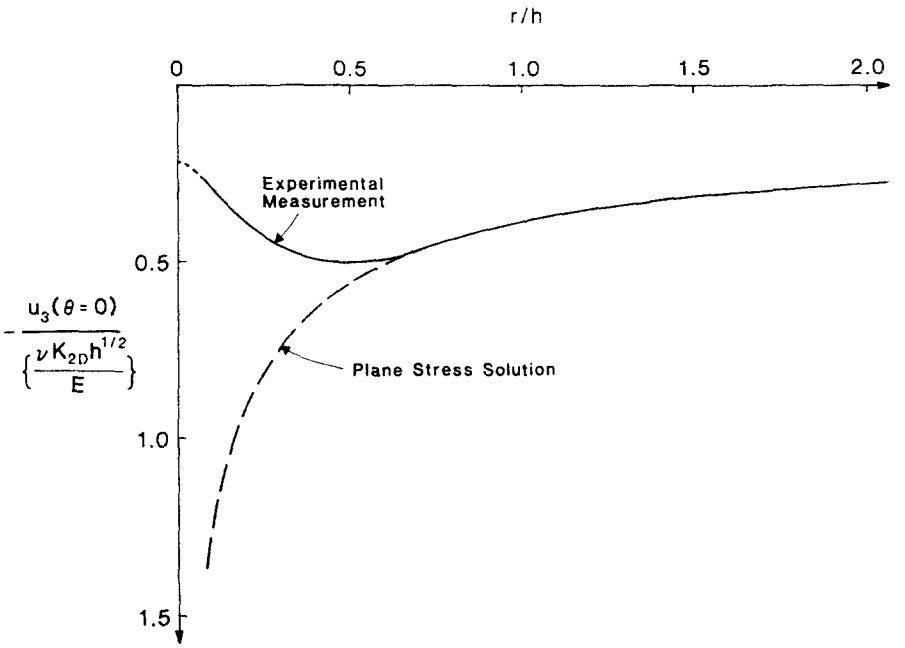

Fig. 7. Normalized out-of-plane displacement, $u_3(x_1, 0, h/2)$, vs distance ahead of the crack tip divided by specimen thickness (obtained by reflected caustics measurements).

that u_3 may not vanish at the crack tip. Further experimental work using interferometry is underway to investigate the details of this region.

The experimental results discussed above are in excellent agreement with the finite-element calculations of Levy, Marcal and Rice[2] and the recent boundary-layer solution of Yang and Freund[1]. Some of the results of [2] are displayed in Fig. 8, where it is demonstrated that σ_{33} approaches zero at $r/h = 0.5$, indicating the establishment of plane-stress conditions at this distance. In the work by Yang and Freund, the state of stress in an elastic plate containing through-cracks is investigated with a view toward assessing the influence of transverse shear on the crack-tip stress and deformation fields. A crack-tip boundary-layer solution is thus obtained, based on the assumption of uniform through the thickness extensional strain. Their results are displayed in Fig. 9 and 10.

In Fig. 9, the nondimensional out-of-plane displacement $u_3(x_1, 0, h/2)$, is plotted vs $(r/\epsilon)^{1/2}$, which is to be compared with our Fig. 7. (ϵ is a length parameter proportional to h.) In Fig. 10, the ratio of $u_3(x_1, 0, h/2)$ and the corresponding plane-stress value is plotted vs $(r/h)^{1/2}$. This ratio is proportional to K^{EXP}/K_{2D} and can be compared to Fig. 6.

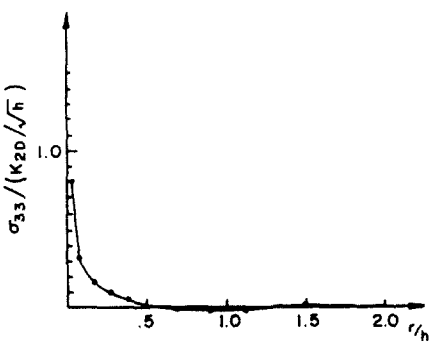

Fig. 8. Variation of midplane σ_{33} with normalized distance from the crack tip (from Levy, Marcal and Rice[2]).

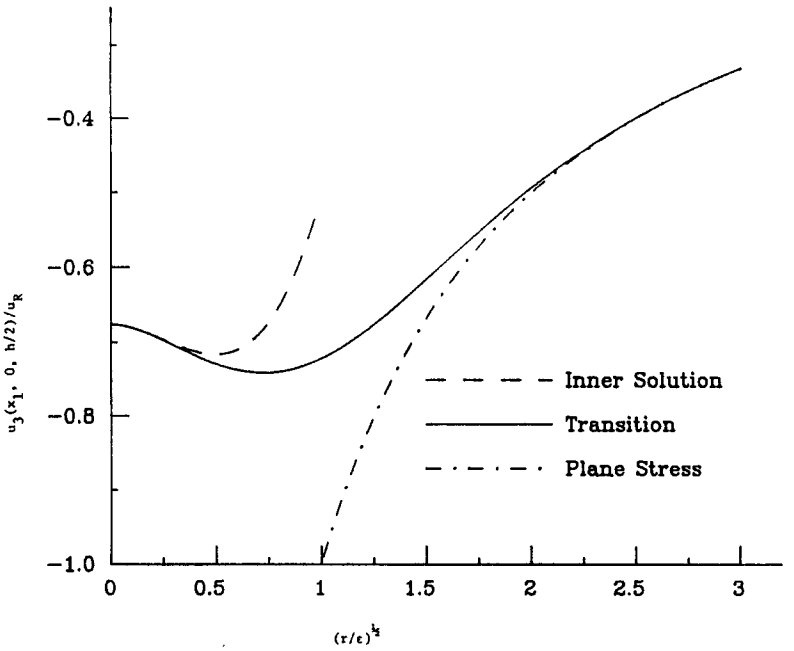

Fig. 9. Normalized out-of-plane displacement, $u_3(x_1, 0, h/2)$ showing inner boundary-layer transition and outer plane-stress regions vs normalized distance from the crack tip. Analytical result by Wang and Freund[1].

The analytical results are in good agreement with the present experiments in a number of issues. In particular, their solution is found to merge smoothly with the plane-stress result, at distances from the tip of one-half the plate thickness. Figure 9 also displays a minimum in the displacement profile, but the location of this minimum is closer to the crack tip than in the present experimental results. Finally, and as demonstrated in Fig. 8, the lateral contraction u_3 on the specimen surface does *not*

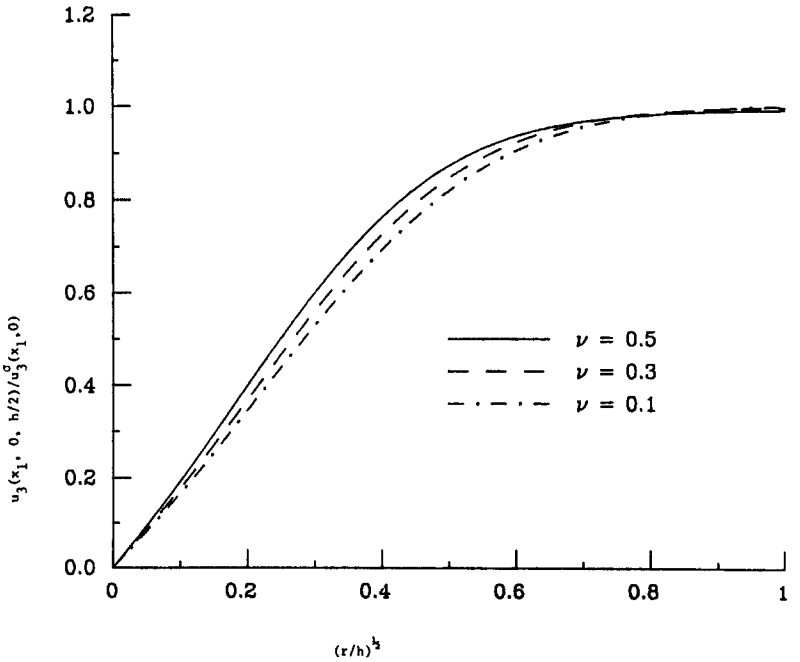

Fig. 10. Out-of-plane displacement derived by corresponding value $u_3^G(x_1, 0)$ or plane stress, vs normalized distances ahead of the crack tip for ν = 0.1, 0.3, 0.5. Analytical results by Wang and Freund[1].

exhibit plane-strain behavior very near the crack tip, "in contrast to what is commonly assumed in problems of this type"[1].

6. SUMMARY AND CONCLUSIONS

1. The three-dimensional nature of the crack-tip field scales with thickness.
2. Plane-stress conditions prevail at distances from the crack tip greater than half the specimen thickness.
3. No significant plane-strain region is observed. Only right at the crack tip ($r/h = 0$), u_3 takes a constant value indicating conditions of generalized plane strain.
4. The r/h dependence of K^{EXP}/K_{2D} suggests that for $0 < r/h < 0.5$ the stress gradients are weaker than the corresponding two-dimensional gradients.
5. The experimental results are consistent with the analysis of Yang and Freund[1] and the numerical results of Levy, Marcal and Rice[2].

Acknowledgements—The authors would like to express their gratitude to Mr. W. Yang and Prof. L. B. Freund of Brown University, for providing them with a copy of their work, as well as the results displayed in Figs. 9 and 10, prior to publication of their work. The authors would also like to acknowledge many helpful discussions with Prof. J. Knowles, Prof. W. G. Knauss and Prof. C. D. Babcock of the California Institute of Technology. The research support of the National Science Foundation, through Grant No. MEA-83-07785, is gratefully acknowledged. One of us (K.R.C.) would also like to acknowledge the support of the National Science Foundation, through Grant No. MEA-8215438, during part of this work.

REFERENCES

1. W. Yang and L. B. Freund, Transverse Shear Effects for Through-Cracks in an Elastic Plate, Brown University Report (1984).
2. N. Levy, P. V. Marcal and J. R. Rice, Progress in three-dimensional elastic–plastic stress analysis for fracture mechanics. *Nucl. Eng. Des.* **17**, 64–75 (1971).
3. E. Sternberg and M. A. Sadowsky, Three-dimensional solution for the stress concentration around a circular hole in a plate of arbitrary thickness. *J. Appl. Mech.* **16**, *Trans. ASME* **71**, 27–38 (1949).
4. J. B. Alblas, Theorie van de driedimensionale spanningstoestand in een doorboovde plaat. Dissertation, Technische Hogeschool Delft, J. J. Paris, Amsterdam, The Netherlands (1957).
5. J. P. Benthem, State of stress at the vertex of a quarter infinite crack in a half space. *Int. J. Solids Structures* **13**, 479–492 (1977).
6. E. S. Folias, On the three-dimensional theory of cracked plates. *J. Appl. Mech. Trans. ASME* **42**, 663–674 (1975).
7. Z. P. Bažant and L. F. Estenssoro, General numerical method for three-dimensional singularities in cracked or notched elastic solids. Proceedings of the 4th International Conference on Fracture, University of Waterloo, *Fracture* **3**, 371–385 (1977).
8. R. J. Hartranft and G. C. Sih, An approximate three-dimensional theory of plates with application to crack problems. *Int. J. Eng. Sci.* **8**, 711–729 (1970).
9. M. L. Williams, On the stress distribution at the base of a stationary crack. *J. Appl. Mech.* **24**, 109–114 (1957).
10. J. Beinert and J. F. Kalthoff, Experimental determination of dynamic stress-intensity factors by the method of shadow patterns. In *Mechanics of Fracture*. (Edited by G. C. Sih), Vol. 7. Noordhoff, London, The Netherlands (1981).
11. H. Tada, P. Paris and G. Irwin, *The Handbook of Stress Intensity Factors*. Del Research Corporation (1973).